Phys. Status Solidi C **8**, No. 3, 733–738 (2011) / **DOI** 10.1002/pssc.201000338

physica status solidi c
www.pss-c.com
current topics in solid state physics

Research on efficiency limiting defects and defect engineering in silicon solar cells - results of the German research cluster SolarFocus

Stephan Riepe[*,1,2], Isolde E. Reis[1,2], Wolfram Kwapil[2], Marie Aylin Falkenberg [3], Jonas Schön[2], Herfried Behnken[4], Jan Bauer[5], Denise Kreßner-Kiel[6], Winfried Seifert[7], and Wolfgang Koch[8]

[1] Materials Research Centre FMF, University of Freiburg, Stefan-Meier-Straße 21, 79104 Freiburg, Germany
[2] Fraunhofer Institute for Solar Energy Systems, Heidenhofstraße 2, 79110 Freiburg, Germany
[3] IV. Physikalisches Institut der Georg-August Universität Göttingen, Friedrich-Hund-Platz 1, 37077 Göttingen, Germany
[4] Access e. V., Intzestraße 5, 52072 Aachen, Germany
[5] Max Planck Institute of Microstructure Physics, Weinberg 2, 06120 Halle, Germany
[6] Institute for Experimental Physics, TU Bergakademie Freiberg, Leipziger Str. 23, 09596 Freiberg, Germany
[7] IHP/BTU Joint Lab, BTU Cottbus, Konrad-Wachsmann-Allee 1, 03046 Cottbus, Germany
[8] KoSolCo, Seitz-Berlin-Str. 10, 91550 Dinkelsbühl, Germany

Received 15 May 2010, accepted 3 June 2010
Published online 23 December 2010

Keywords silicon, solar cells, defects, transition metals

* Corresponding author: e-mail stephan.riepe@ise.fraunhofer.de, Phone: +49 761 4588 5636, Fax: +49 761 4588 9250
Web: www.solarfocus.org

Defects in multicrystalline silicon for photovoltaic applications and their impact on solar cell parameters have been investigated in the material research network project SolarFocus. A series of multicrystalline silicon ingots of ultrapure feedstock material were cast with intentional addition of typical transition metal impurities (Fe, Cu, Cr) and Ge as doping elements. The results of lifetime measurements, NAA and FTIR analysis, solar cell processing and microscopic investigations are presented in this study. For ingots intentionally contaminated with transition metals, the combined analysis reveals that despite the overall high impurity content, good solar cell efficiencies can be reached. A strong influence of the in-diffusion of metal impurities from the crucible as well as the back-diffusion from the top region of the ingot ca still be observed. All metals show a strong precipitation behaviour throughout the whole ingot. The solar cell efficiency is both limited by multiple recombination active defects and shunts, induced by a high metal contamination via indirect mechanisms. Solar cells with efficiencies up to 15.2 % for material contaminated with 20 ppma Fe in the melt, 15.7 % for 20 ppma Cu and 15.1 % for 20 ppma Cr were processed. A positive effect of Cu added to the feedstock could not be found. Ge-rich ingots showed strong effects of increasing silicon carbide and silicon nitride formation with increasing Ge content larger than 0.5 wt.% thus reducing solar cell efficiency.

1 Introduction Impurities in silicon can drastically modify the material properties relevant for solar cells made out of silicon wafers in different ways. Transition metal impurities such as iron, copper and chromium are known to enhance the net recombination of minority carriers within the bulk material or negatively influence the emitter region and thus are detrimental for the cell efficiency [1]. In contrast, elements such as germanium are investigated as dopants for monocrystalline silicon in semiconductor industry in order to positively influence the internal gettering characteristics [2]. However, the production of solar cells from Si_xGe_y-alloys with Ge-content up to 16 at.% proved rather difficult [3]. The knowledge about defect interactions and their relative importance in the face of mul-

tiple impurities, which are inadvertedly present in solar cell material, is of utmost interest for the use of alternative feedstock materials such as upgraded metallurgical silicon (UMG-Si) feedstock [4,5] and for the improvement of actual industrial materials for solar cell production. Therefore, multicrystalline silicon (mc-Si) materials with well defined impurity concentrations have been crystallized and subsequently characterized with a set of different methods to investigate interactions of metal impurities, dopants and microstructural defects. Thus the incorporation mechanisms and limits of tolerable amounts of impurities in solar silicon could be analysed. The platform for this research has been the SolarFocus-project, a German-based joint venture project consisting of twelve industry partners and twelve universities/research institutions in the field of silicon photovoltaics [6].

2 Experimental approach For the investigation of the effect of Fe, Cu, Cr and Ge introduced into mc-Si material either in the feedstock itself or during crystallization, a series of experimental mc-Si ingots have been grown by the directional solidification (DS) technique with a solidification velocity of 1.0–1.1 cm/h in an experimental casting furnace at Deutsche Solar AG [7]. The feedstock was melted in a quartz crucible and cast into a rectangular solidification crucible, coated with industrial quality Si_3N_4 lining. The ingots generated two bricks of 125 mm side length or one brick of 156 mm side length with three sides influenced by indiffusion of impurities from the crucible system, the fourth side having a distance of 80 mm to the crucible. In order to minimize cross contamination of added impurities, three different melting crucibles were used. The block height was between 200 mm and 220 mm. Table 1 gives an overview over the investigated ingots.

Table 1 Overview of ingots with intentionally added elements

	Ingot description	Added elements
(1)	reference ingot	pure Si feedstock
(2)	low iron level	2 ppma Fe
(3)	high iron level	20 ppma Fe
(4)	high copper level	0 ppma Fe, 20 ppma Cu
(5)	low iron, high copper level	2 ppma Fe, 20 ppma Cu
(6)	high iron, high copper level	20 ppma Fe, 20 ppma Cu
(7)	high chromium level	20 ppma Cr
(8)	reference ingot 2	pure Si feedstock
(9)	low germanium level	0.5 wt.% Ge
(10)	medium germanium level	1.0 wt.% Ge
(11)	high germanium level	2.0 wt.% Ge

In two reference ingots, ultrapure feedstock was intentionally doped with boron to give a material with a resistivity of about 0.7-1 Ωcm throughout the entire ingot. In five other ingots, Fe, Cu and Cr in form of small discs of pure elemental metal were added to the B-doped feedstock aiming at a lower concentration level (2 ppma Fe or Cu) or a higher concentration level (20 ppma Fe, Cu or Cr) in the melt or combinations thereof. Thus the interaction between metal impurities and their precipitation behaviour with respect to microstructural defects could be studied. In a second series of ingots, pure metallic germanium was added to the feedstock in three concentration levels. Bricks of 125 mm or 156 mm side length were cut out of each ingot and subsequently wafered. Every 10th wafer was processed into a solar cell by an industrial-type cell process with an emitter indiffused via a gas phase process and screen printed back contacts [7]. Lifetime measurements and other electrical and microstructural analyses were performed on brick and wafer level. A vertical slab of 3 mm thickness perpendicular to the long side of the ingot was cut for Infra Red Microscopy (IRM) and Fourier Transform Infrared Spectroscopy (FTIR) measurements. From the remaining material, analytical samples from seven to eight different block heights for Neutron Activation Analysis (NAA) were prepared.

3 Influence of iron, copper and chromium

3.1 Metal distribution Figure 1 shows the profiles of the total Fe (upper diagram) and Cu content (lower diagram), measured by height-dependent NAA.

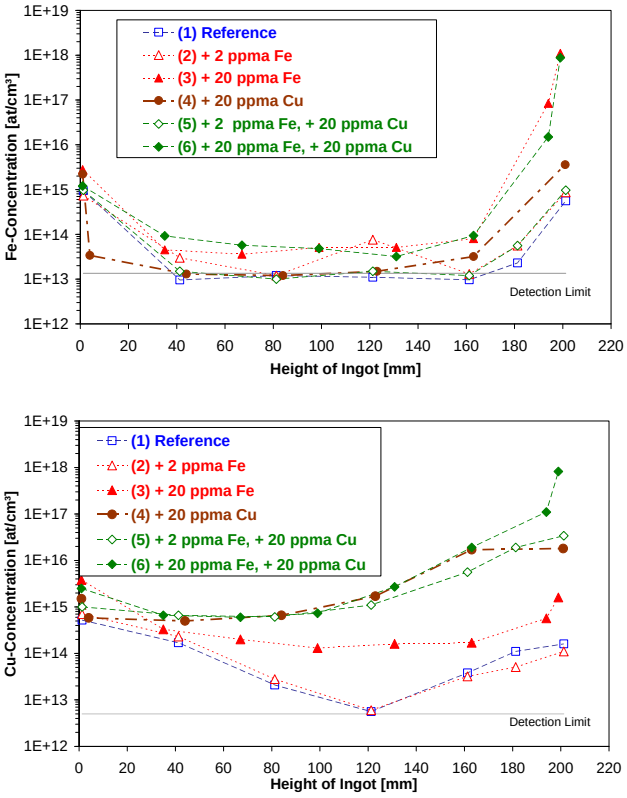

Figure 1 Height-dependent total Fe (top) and Cu (bottom) concentration profiles, measured by NAA method.

Concentrations for Cr and Ni were measured as well for all ingots (not shown here). They are within a range of 3×10^{11} at/cm^3 to 2×10^{14} at/cm^3 for Cr and 8×10^{12} at/cm^3 to 5×10^{14} at/cm^3 for Ni. In all profiles, a mixture of transition metals was found independent of intentional contamination. For all ingots, profiles for the evaluated transition metals showed similar values at the block bottom: 7-13$\times10^{14}$ at/cm^3 for Fe, 5-14$\times10^{14}$ at/cm^3 for Cu, 1-12$\times10^{13}$ at/cm^3 for Cr and 2-12$\times10^{13}$ at/cm^3 for Ni. The Cu profile in ingot (3) and the Fe profile in ingot (4) are located in between two groups of profiles with high and low concentration levels. This may point to an interaction between Fe and Cu, but a cross contamination for these ingots cannot be ruled out.

The height-dependent total impurity content was modeled by taking four different mechanisms into account [8]:
(i) Incorporation of impurities into the crystal with initial concentration c_0 in the melt is described by the Scheil model [9] with an effective segregation coefficient k_{eff} .
(ii) Crucible and lining of industrial production quality act as sources of metal impurities [10]. Thus, impurities can be continously incorporated into the melt over crystallization time, modeled by an effective transfer rate.
(iii) After solidification, mobile species diffuse from the crucible through the lining into the solidified crystal.
(iv) Diffusion from the utmost top of the block with very high impurity concentration back into the block volume occurs directly after solidification. It can be modeled by a solid state diffusion and can significantly differ for slow and fast diffusing elements.

The upper diagram in Fig. 2 shows the simulated and measured profile for the total Fe concentration in ingot (3) with 20 ppma Fe added to the feedstock. The shape of the simulated profile in the upper part is due to back-diffusion and simulated precipitation of Fe based on the Fokker Planck Equation [8]. The segregation coefficient is found to be $k_{eff,\,Fe}$(multi) = 1.7-2.2$\times10^{-5}$, which is 3-4 times higher than literature data for monocrystalline silicon $k_{eff,\,Fe}$(mono) = 5-7$\times10^{-6}$ [11,12]. It has been discussed that this might be due to an increased incorporation of Fe at areas with high density of structural defects [13]. Modeling via an increased solid solubility in combination with precipitation can describe the data [8], but thermodynamical considerations imply a more complex mechanism. Whereas the interstitial iron concentration Fe_i in the block middle is on the order of a factor 10 lower than Fe_{total}, in the top and bottom region, this factor can be as high as 200 due to in- and backdiffusion in the crystal [7,8].

The lower diagram in Fig. 2 displays the simulated Cu profile for ingot (5) without a specific precipitation model, together with NAA data points of ingots (4)-(6). The diffusion regions at block bottom and top are largely extended due to the high diffusion coefficient of Cu in the silicon crystal in comparison to Fe [14]. For ingots (1) and (2), where no metallic Cu was initially added to the feedstock, in-diffusion from the crucible and back-diffusion from the top dominate the whole profile (see also Fig. 1).

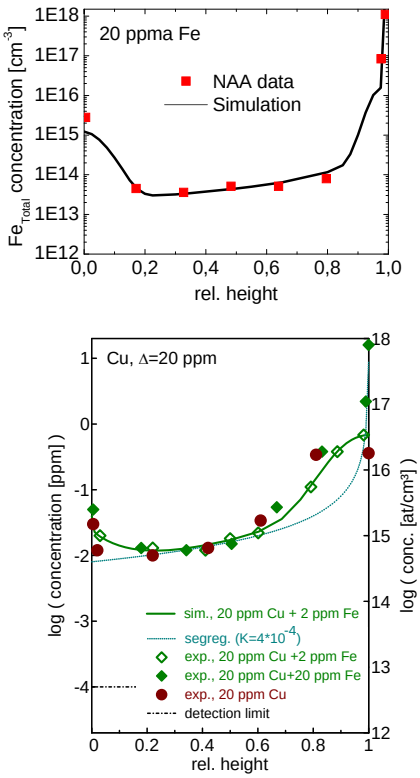

Figure 2 Modeling of height dependent profiles for total metal concentration of Fe (upper diagram) and Cu (lower diagram).

The applied effective segregation coefficient $k_{eff,\,multi}$(Cu) = 4×10^{-4} is in good agreement with literature values for mono-Si.

Evaluation of the Cr concentration in ingot (7) yields an effective segregation coefficient $k_{eff,\,multi}$(Cr) = 5×10^{-6} and a profile comparable to Fe in ingot (3).

3.2 Oxygen and carbon distribution Height-dependent measurements of the interstitial oxygen concentration O_i showed a decrease from bottom to top in accordance with the segregation mechanism (see Fig. 3).

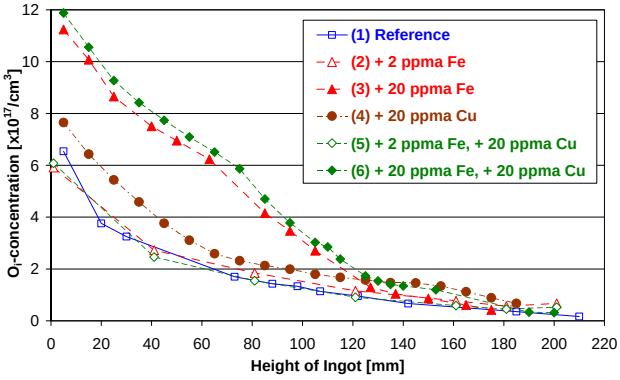

Figure 3 Height dependent O_i-profiles, measured by FTIR on vertical slabs.

While the addition of Cu in ingots (4) and (5) is leading to an increase in the O_i-content by up to 40%, the addition of a high amount of Fe results in more than doubling the O_i-content in the bottom half of both ingots with 20 ppma metal content. Please note, that the total oxygen content might be significantly higher.

FTIR measurements of substitutional carbon C_s show an almost linear increase from 1.2×10^{17} at/cm^3 at the block bottom to 7.6×10^{17} at/cm^3 at 180 mm block height. Whereas in the reference material, C_s concentration in the block top higher than 180 mm is above 10^{18} at/cm^3, it significantly drops for ingots (2) and (5) with additional metal impurities.

3.3 Precipitates It is generally known that most of the oxygen in the silicon matrix is bound as precipitates surrounded by its interstitial species O_i. Large quantities of iron seem to alter the precipitation behaviour of oxygen directly or indirectly (see Fig. 3). Interactions with crystal defects or iron precipitates probably play a role for this effect. Our results suggest that these mechanisms are not present in silicon only contaminated with Cu.

In the top parts of all ingots, IRM analyses find SiC and Si_3N_4 precipitates in varying densities. In the reference material, a zone with high density of precipitates is found above 190 mm block height. For ingot (2), this zone is found to begin at a significantly lower block height of approx. 180 mm correlating with the reduction of C_s at this position. Interestingly, the amount of precipitates found in the top of ingot (5) is less than in ingot (2).

In the top regions of ingots (5) and (6), star-shaped and dot-shaped precipitates of $FeSi_2$ and Cu_3Si were identified by IRM and EBIC analyses [7] (see Fig. 4 left). TEM characterization reveals, that either single $FeSi_2$ or Cu_3Si appear as individual precipitates, or both metal silicides are colocated, meaning that they are found at the same location. A ternary phase of Fe_xCu_ySi does not seem to form. Interestingly, some colocated precipitates with oxygen on the interface layer between Cu_3Si and the silicon matrix were found (see Fig. 4 right).

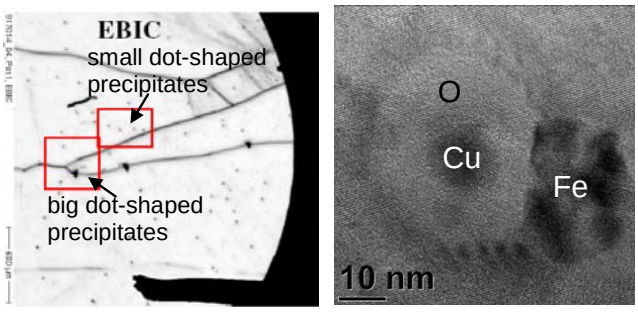

Figure 4 EBIC image (left) of dot-shaped precipitates and TEM image (right) of colocated precipitates with oxygen surrounding the Cu_3Si precipitate, found in ingots with additional Fe and Cu.

3.4 Solar cell analysis Fig. 5 shows cell efficiencies over block height of the highly metal contaminated ingots in comparison to the reference material. Efficiencies up to 15.2 % for material contaminated with 20 ppma Fe and 15.7 % for 20 ppma Cu were be reached. A discussion of the height dependent open circuit voltage V_{oc} and efficiency η results of all ingots is given in [7]. The efficiency limit for the applied solar cell structure and processing sequence on the experimentally cast reference material was 16.1 % for ingot (1) and 15.3 % for ingot (8), indicating significant material variations over the whole experiment. All solar cells out of intentionally contaminated material show lower efficiencies.

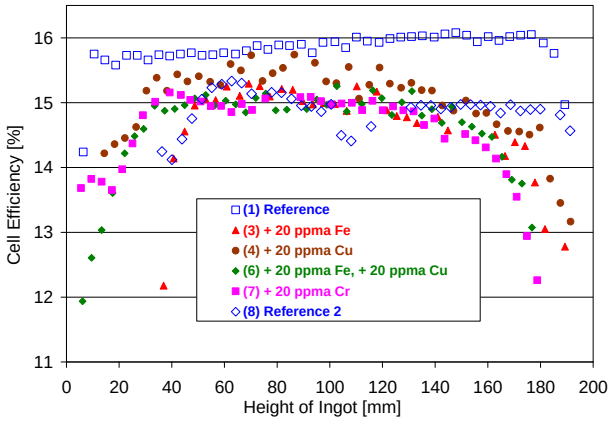

Figure 5 Height dependent cell efficiency profiles of reference ingots and ingots with addition of 20 ppma metal impurities – work done at Sunways, Arnstadt.

In addition to the evaluation of efficiency, reverse bias characteristics of cells from metal contaminated material were investigated. It was found, that a secondary effect of metal precipitates consists in the induction of soft diode breakdown [15]. This may result in a severe reduction of the solar module lifetime in case that so called hot-spots develop, and has to be taken into account for the assessment of tolerable amounts of metal in the feedstock.

3.5 Discussion For the assessment of the influence of metal impurities on the efficiency for solar cell production, a normalized efficiency defined as the product of V_{oc}, I_{sc} and a scaling factor, representing a fill factor of 0.78, is shown as a function of the total metal content measured via NAA (see Fig. 6). Thus technological problems related to a varying fill factor are taken out of consideration here. However, it has to be noted that the fill factor itself might strongly be influenced by the material properties. The limitation by the applied cell structure and cell process is indicated by the shaded region with upper limit of 16.1 %.

A total Fe concentration in the crystallized material above approx. 2×10^{13} at/cm^3 starts limiting the cell effiency, with an increasingly severe reduction for Fe concentrations higher than 1×10^{14} at/cm^3. Taking the effective segregation

coefficient for these experiments into account and evaluating only material not influenced by in-diffusion from the crucible in the block bottom, a concentration of up to 1.2×10^{17} at/cm^3 of iron in the feedstock material (equivalent to 2.4 ppma) would yield solar cell efficiencies comparable to standard material from the block middle up to 90% block height. Depending on the crystallization process and contamination level, reduced efficiencies in the block bottom may account for about 10–15 % of ingot height (see Fig. 5). Thus up to 75-80 % of the ingot material could yield solar cells with efficiencies higher than 15 %.

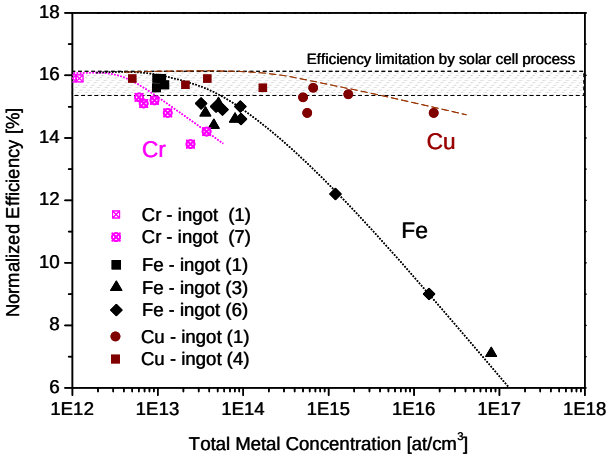

Figure 6 Normalized cell efficiency plotted versus total metal concentration. The lines serve as guides to the eye.

With an analogous argumentation, a Cu concentration of about 3×10^{14} at/cm^3 on wafer level and thus about 9×10^{16} at/cm^3 in the feedstock (equivalent to 1.8 ppma), or a Cr concentration of about 3×10^{12} at/cm^3 and 6×10^{16} at/cm^3 (equivalent to 1.2 ppma), respectively, would lead to the same results. Since this evaluation does not distinguish between interstitial or precipitated metal atoms and thus cannot judge secondary effects as induced by deformation of the silicon matrix and dislocation generation, these values give only a qualitative estimation. The value for Cu is in good agreement with results presented by Rohatgi et al. [16]. The deviation in the assessment of Fe may be due to the assessment of total metal content and a higher efficiency limit for this study. Contrary to postulations in literature [17], a positive effect of the addition of Cu to the feedstock in presence of other metal impurities could not be found.

4 Solar cells on germanium doped mc-Si

The internal gettering behaviour in Czochralski grown silicon, which is exploited in semiconductor technology, can be enhanced by Ge doping of up to 2 ppma [2]. In order to investigate a proposed positive influence of Ge on solar cell efficiency [3], a series of three mc-Si ingots with addition of Ge was cast (see Table 1) and processed.

4.1 Material analysis Height-dependent profiles of Ge concentration, measured by NAA for the ingots with 0.5 wt.% and 1.0 wt.%, could be modeled with an effective segregation coefficient of $k_{eff,\,Ge}$ (multi) = 0.32. Infrared microscopy analysis and minority carrier lifetime mapping on a vertical cross section of ingot (10) show pronounced inhomogeneities over block height (Fig. 7 and 8).

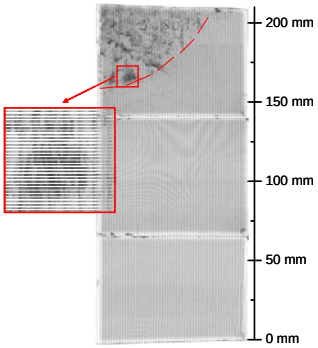

Figure 7 Microscopy analysis of vertical slab of ingot (10) of 205 mm height with 1 wt.% Ge showing high precipitate density in upper block part.

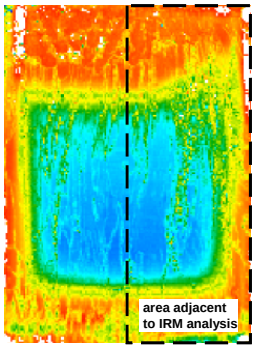

Figure 8 Lifetime mapping of unpassivated adjacent brick (blue colour indicates high lifetime, red colour indicates low lifetime values).

A significant reduction in lifetime starting above 75% block height in ingot (10) correlates with a region of high density of Si_3N_4 and SiC precipitates which were identified by IRM analyses. The curved shape of the interface zone reflects the non-planar liquid-solid interface for this specific crystallization and block height. A similar region is found in ingot (9) starting at 82 % block height in combination with shaded regions in the block bottom, visible by IR inspection. Strong shading is also found in the bottom region of ingot (11) and a high density of SiC and Si_3N_4 above 57 % block height. No shading or regions of high inclusion density were observed in a reference ingot without added Ge. FTIR measurements (Fig. 9) of C_s show a significant reduction above these heights in ingot regions with pronounced SiC and Si_3N_4 precipitate formation.

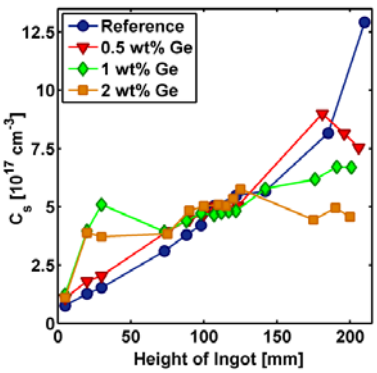

Figure 9 Height-dependent C_s profiles for ingots with up to 2 wt.% of Ge added to the feedstock, measured by FTIR.

4.2 Solar cell characterization and discussion

Solar cells processed from ingot (9) and (10) possess cell efficiencies in the middle of the ingots of up to 16.1 % comparable to results of the reference material (see Fig. 5) and are not shown here. Significant efficiency reduction correlates with the aforementioned regions of high precipitate density and shading. The reverse bias characterisitic of cells from these regions, analysed by Dark Lock-In Thermography DLIT, show areas of high local current flow identifying ohmic shunts. The IV-characteristics indicate material induced shunts caused by SiC filaments [18].

Additionally, SiC precipitates can introduce dislocations and stress into the silicon matrix. Since there is always a certain amount of transition metals in the melt due to the influence of the crucible system, these metals inevitably decorate microstructural defects and can form metal precipitates. In combination with residual stress around these defects, high recombation activity occurs resulting in low lifetime and thus solar cell efficiencies.

SiC clustering seems to be amplified above a certain threshold concentration of Ge in the Si melt thus impairing solar cell properties. NAA measurements reveal that this effect starts at a Ge concentration of approx. 0.5 wt.% in the crystal. Therefore a concentration ≤ 0.3 wt.% of Ge in the feedstock should be maintained in order to avoid regions with high precipitate density up to 90 % block height for a similar crystallization process. An increase in lifetime due to a reduced dislocation density could not be observed. Based on this study and literature values, a possible increase in solar cell efficiency by addition of Ge to the silicon feedstock would be expected in a region of about 10^{17}-10^{19} at/cm^3 equivalent to 5–500 ppmw.

5 Conclusions

The combined analysis of material and solar cells reveals a complex picture of defects in intentionally metal contaminated materials. Only high levels of contamination of transition metals in the range of 20 ppma in the melt result in significant higher impurity levels in the middle of the ingots and thus reduce solar cell efficiencies. Strong interactions in the precipitation of different species are found. Our results imply, that feedstock containing 1-2 ppma of the investigated metal impurities is able to yield solar cells with efficiencies up to 16 %. The in-diffusion of metal impurities from the crucible as well as the back-diffusion from the top of the block dominate the impurity profiles for standard as well as lightly contaminated mc-Si material. In combination with microstructural defects induced by the crystallization process, these impurities limit the solar cell efficiencies. A positive effect on solar cell efficiency by addition of Cu to the feedstock could not be found.

Mc-Si ingots with up to 2 wt.% Ge showed increased precipitate density and reduced solar cell efficiencies in the upper block parts with Ge concentration larger than approx. 0.5 wt.%. An increase in cell efficiencies could not be observed for material with a Ge content of 0.5 wt.% or above in the feedstock.

Acknowledgements The authors would like to thank all partners for their contribution, especially K. Hesse and L. Fabry, Wacker Polysilicon, for high purity feedstock, C. Knopf and B. Gründig-Wendrock, SolarWorld, Freiberg, for casting of ingots, material preparation and electrical measurements, and M. Braun, Sunways Production GmbH, Arnstadt, for solar cell processing. The network project has been financially supported by the German Federal Ministry for the Environment, Nature Conservation and Nuclear Safety (BMU) within the research cluster SolarFocus (0327650) and by all the industry partners.

References

[1] G. Coletti, P.C.P. Bronsveld, C. Knopf, C.C. Swanson, R. Kvande, L. Arnberg, H. Habenicht, and W. Warta, in: Proceedings 24th European Photovoltaic Solar Energy Conference, Hamburg, Germany (2009), pp. 1011-1014.
[2] J. Chen, D. Yang, X. Ma, D. Que, Mater. Sci. Eng. B **159/160**, 235-238 (2009).
[3] P. Raue, A. Lawerenz, L. Long, M. Rinio, E. Buhrig, and H.J. Möller, in: Proceedings 14th European Photovoltaic Solar Energy Conference, Barcelona, Spain, 1997, pp. 1791-1794.
[4] S. Pizzini, Appl. Phys. A **96,** 171-188 (2009).
[5] J. Libal, S. Novaglia, M. Acciarri, S. Binetti, R. Petres, J. Arumughan, R. Kopecek, and A. Prokopenko, J. Appl. Phys. 104, 104507 (2008).
[6] S. Riepe, I.E. Reis, and W. Koch, in: Proceedings 23rd European Photovoltaic Solar Energy Conference, Valencia, Spain, 2008, pp. 1410-1413.
[7] I.E. Reis, S. Riepe, W. Koch, J. Bauer, S. Beljakowa, O. Breitenstein, H. Habenicht, D. Kreßner-Kiel, G. Pensl, J. Schön, and W. Seifert, in: Proceedings 24th European Photovoltaic Solar Energy Conference, Hamburg, Germany 2009, pp. 2144-2148.
[8] J. Schön, H. Habenicht, M.C. Schubert, and W. Warta, Solid State Phenom. **156-58**, 223-228 (2010).
[9] E. Scheil, Z. Metallkd. **34,** 70-72 (1942).
[10] E. Olsen and E. J. Øvrelid, Prog. Photovolt.: Res. Appl. **16**, 93-100 (2008).
[11] J. R. Davis et al., IEEE Trans. Electron Devices **27**, 677 (1980).
[12] H. Lemke, in: Semiconductor Silicon, edited by H. R. Huff et al. (The Electrochemical Society, New Jersey, USA, 1994), p. 695.
[13] D. Macdonald et al., J. Appl. Phys. **97,** 33523-1-7 (2005).
[14] K. Graff, Metal Impurities in Silicon-Device Fabrication. 2nd ed., Springer Ser. Mater. Sci., Vol. 24, edited by R. Hull et al. (Springer, Berlin, 1999), p. 28.
[15] W. Kwapil et al., Appl. Phys. Lett. **95**, 232113 (2009).
[16] A. Rohatgi et al., Solid-State Electron. **23**, 415-422 (1980)
[17] T. Buonassisi et al., Acta Materialia **55,** 6119-6126 (2007).
[18] O. Breitenstein, J. Bauer, and J.P. Rakotoniaina, Semiconductors **41**, 440-443 (2007) (ISSN 1063-7826).

